

Photochemical oxidation of chrysene at the silica gel–water interface

Li Kong, John L. Ferry*

Department of Chemistry and Biochemistry, University of South Carolina, Columbia, SC 29208, USA

Received 4 June 2003; received in revised form 5 September 2003; accepted 9 September 2003

Abstract

The photolysis of chrysene at the silica–water interface proceeds more efficiently than when dissolved in solution. Loss of chrysene was apparently through self sensitized oxidation by singlet oxygen. The role of singlet oxygen in the system was probed by application of the $^1\text{O}_2$ scavenger, 1,4-diazabicyclo[2,2,2]-octane (DABCO). The initial rate of chrysene loss exhibited a positive correlation with chrysene loading ($\mu\text{mol g}^{-1}$) on silica gel supports. The system was subjected to model environmental conditions (simulating seawater) and the effects of halide ions on the photodegradation process were determined. Singlet oxygen steady state concentrations were measured under all experimental conditions by using 2,5-diphenylfuran as a singlet oxygen trapping agent, and varied from $(3.73 \pm 0.37) \times 10^{-12}$ to $(1.43 \pm 0.14) \times 10^{-11}$ M under our experimental conditions. $[^1\text{O}_2]_{ss}$ was a function of chrysene loading and salinity; high chrysene loading promoted high singlet oxygen concentrations, but high salinity suppressed it.

© 2004 Elsevier B.V. All rights reserved.

Keywords: Photochemical oxidation; Chrysene; Silica gel–water interface

1. Introduction

The photochemical oxidation of PAHs at the silica gel–air or organic solvent interface has been well-studied [1–4]. The photoexcitation of PAHs is known to produce highly reactive, long lived triplet states [5–7]. In solution, $^3\text{PAHs}$ are known to dimerize, photoionize, or engage in energy transfer reactions (often with dissolved $^3\text{O}_2$, yielding $^1\text{O}_2$) [4,8–10]. Sigman et al. found that the direct photolysis of acenaphthylene in aerated aqueous solutions resulted in the formation of the *cis* and *trans* dimers [9], and reported the photoionization of pyrene in aqueous solution (based on careful product analysis) [8]. Fasnacht and Blough also suggested photo-induced electron transfer from PAHs to H_2O or O_2 in dilute solution [11]. Gollnick reported the production of singlet oxygen from excited PAHs by energy transfer could lead to the degradation of the sensitizing PAH [12]. These proposed mechanisms have received a great deal of support in the peer reviewed literature, and some excellent reviews on this chemistry have been published [4,8,9,13–15]. Generally, the PAH photodegradation mechanism seems to be a concentration-dependent process. In dilute solutions (submicromolar), photoionization probably dominates [9,11]; at higher concentrations, it is possible for PAHs to photodegrade through reaction of the PAH with

singlet oxygen (a self-sensitized process) [16,17]. This difference in mechanism can be explained by the short (2 μs) [18] lifetime of $^1\text{O}_2$ in H_2O . At concentrations $<1\text{--}10 \mu\text{M}$, it is unlikely that $^1\text{O}_2$ can diffuse far enough in water to encounter another PAH to react with before relaxing to the ground state. In this study, we investigated how adsorption on a surface (at high local concentrations) affects the photolysis of chrysene in aqueous solution (where its low solubility would normally rule out $^1\text{O}_2$ chemistry).

2. Experimental details

2.1. Chemicals

Chrysene (98%), 1,4-chrysenequinone, phthalic acid (99.5%), methyl salicylate and 1,4-diazabicyclo[2,2,2]-octane (DABCO) (98%) were purchased from Aldrich. 2-Formyl benzoic acid ($>98\%$) was purchased from TCI. 2,5-Diphenylfuran was purchased from Alfa Aesar. Instant Ocean™, methanol (GC grade) and *n*-pentane (pesticide grade) were supplied by Fisher. Methyl-*t*-butyl ether (MTBE, GC grade) was supplied by Merck KGaA, Germany. Silica Gel 60 was purchased from EM Science. The N_2 BET surface area of Silica Gel 60 was $453.0 \pm 0.4 \text{ m}^2/\text{g}$ with the particle size of $\leq 63 \mu\text{m}$ and pore diameter of 60 Å. Acetone was dried over anhydrous sodium sulfate. All other materials were used as received.

* Corresponding author. Tel.: +1-803-777-2646; fax: +1-803-777-9521.
E-mail address: ferry@mail.chem.sc.edu (J.L. Ferry).

The standard for 1,4-chrysenediol was obtained by the NaBH_4 reduction of 1,4-chrysenequinone [19]. Following reduction, the air sensitive 1,4-chrysenediol was immediately derivatized with BSTFA, using the method described by Li et al. [20].

2.2. Experimental setup and methods

Reactions were carried out in a Pyrex air tight reactor illuminated by a 1000 W Xe arc lamp filtered through a Pyrex water jacket (supplemental). All handling of chrysene solutions was done under yellow light. The deposition of chrysene onto silica gel (unactivated) was achieved by the *n*-pentane slurry method described by Dabestani and coworkers [1,3,21]. Chrysene loading was determined by extracting deposited chrysene from silica gel (a known mass of silica gel in a known volume of solvent) and quantifying it by GC–MS techniques. Co-deposition of DABCO or 2,5-diphenylfuran was achieved by modifying the method of Dabestani and coworkers to include those reagents in the pentane stock at the desired molar ratio [1,3,21].

For solution phase photochemical studies, aqueous chrysene was prepared by spiking 10.00 ml chrysene in methanol stock solution into 90.00 ml 0.001 M NaHCO_3 buffer or simulated seawater (Instant OceanTM) over a range of different salinities, making the final irradiated solution 10% MeOH, an approach consistent with the work of Miller and Olejnik [22]. The corresponding heterogeneous experiments were prepared by taking up silica gel precoated with chrysene into 100 ml buffer or simulated seawater at the desired salinity and suspending it with vigorous mixing.

All experiments were allowed to equilibrate in the dark with stirring for 50 min before illumination. pH was monitored during equilibration and was adjusted to 8.30 with 0.1 M HCl or NaOH. Following equilibration, the lamp was ignited, and illumination of the reactor commenced when lamp output stabilized (15 min after the light was on). Samples (2 ml) were removed from the top sample port with a 4 ml spring loaded syringe (Manostat). Samples were immediately placed in amber EPA vials precharged with 2 ml of MTBE (with triphenylmethane internal standard). Samples were sonicated for 10 min and then extracted on a vortex mixer for 1 min. The organic layer was removed and stored at 4 °C until analysis by GC–MS.

2.3. Instrumental

Fluorescence spectra were recorded by a SLM-Aminco Model 8100 spectrofluorometer (Spectronic Instruments, Rochester, NY, USA) equipped with a 450 W ozone-free xenon arc lamp and an R-928 photomultiplier. The slit-width for both the excitation and emission monochromators was set to give a 2 nm spectral resolution.

All GC analyses were done on a Varian 3800 GC equipped with an 8200 autosampler and a Saturn 2000 IT-MS. The analytical column was J&W DB-5MS ($L = 30$ m, i.d. =

0.25 mm, d.f. = 0.25 μm) column. Carrier gas was He, and the flow rate was 1.3 ml min^{-1} . The injector port was set for splitless operation at 250 °C. The autoinjector volume was set at 1 μl . The temperature program and the data acquisition parameters have been described previously (supplemental).

2.4. Product determination

1,4-Chrysenequinone was extracted and identified without derivatization. 1,4-Chrysenediol was extracted by MTBE, concentrated by cool evaporation, re-dissolved in acetone, and derivatized with BSTFA at room temperature [20]. 2-Formylbenzoic acid, phthalic acid and 2-hydroxybenzoic acid were extracted at pH 1, and the organic extract was derivatized with CH_2N_2 to yield the corresponding methyl esters [19,23]. All were positively identified by comparing their retention time and mass spectra against those of standards.

3. Results and discussion

3.1. Distribution of chrysene on SiO_2

The emission spectrum of chrysene coated on silica (aqueous suspension) was compared to that obtained from MTBE, excitation at 270 nm (Fig. 1). The fluorescence spectra did not reveal contributions from excimer or excimer-like emissions (PAH excimers are usually centered 400–550 nm) [8,24] which implied that chrysene was distributed on the silica gel surface in a manner that did not allow significant π – π interaction. The spectra were red-shifted by approximately 6–7 nm in aqueous silica gel slurry relative to in MTBE solution. The differences between the emission spectrum of free and adsorbed chrysene are probably a result of simple adsorption to the silica surface [25,26], however, it is also possible that chrysene was present on the surface in some kind of aggregate (although not in a configuration that permitted excimer formation).

3.2. Photolysis of chrysene at silica gel–water interface (0.001 M NaHCO_3)

Chrysene photodegradation was apparently first order in chrysene, with an experimental rate constant (k_{obs}) of $(0.60 \pm 0.06) \times 10^{-2} \text{ min}^{-1}$. The addition of silica gel (1.0 wt.%) caused an increase in k_{obs} of approximately a factor of 2, to $(1.31 \pm 0.13) \times 10^{-2} \text{ min}^{-1}$ (Fig. 2). When chrysene was introduced pre-adsorbed to silica gel, at a loading of 6.43 $\mu\text{mol g}^{-1}$ (the total number of moles of chrysene/unit volume was the same in both experiments), the photodegradation rate was the same as that when silica gel was introduced separately (within experimental error). The total chrysene loading in the heterogeneous system exceeded chrysene's aqueous solubility ($1.3 \times 10^{-2} \mu\text{M}$ [27]) by a factor of 5×10^3 , implying that the “local concentration” of

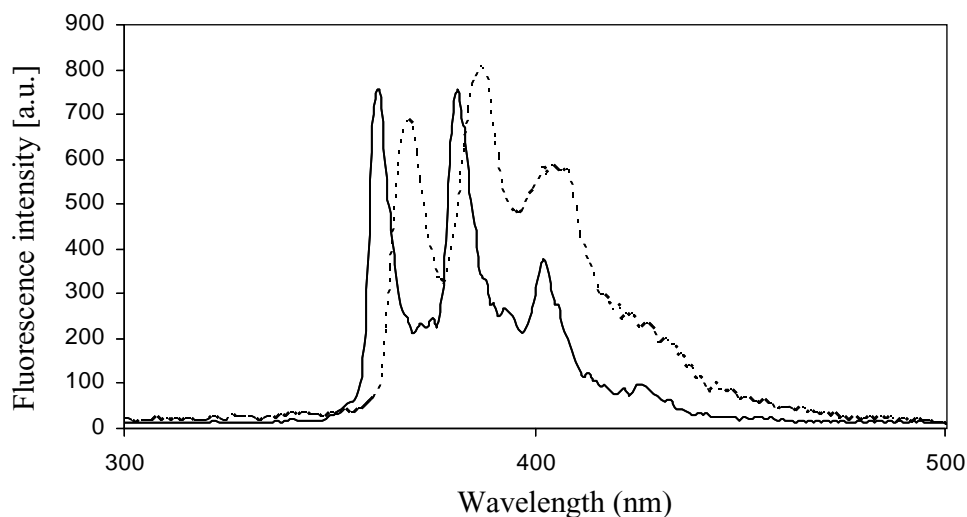


Fig. 1. The emission of chrysene is red-shifted by approximately 6 nm in aqueous silica slurries relative to solution. Excitation: 270 nm; (—) MTBE solution ($6.42 \mu\text{M}$); (---) silica gel suspension (0.001 M NaHCO_3); pH: 8.30; chrysene loading: $4.53 \mu\text{mol g}^{-1}$; SiO_2 : 1 wt.%.

chrysene around the silica surface was high compared to its concentration in the aqueous phase. In such an environment, there should be more opportunities for collision between $^1\text{O}_2$ and chrysene, affording a higher apparent rate of reaction.

The surface-enhanced photodegradation of PAHs has been observed before. Sigman and Zingg have reported that the addition of SiO_2 particles to solutions of anthracene in cyclohexane increased the rate of anthracene photolysis by a factor of 6.5 under argon and a factor of 56 under oxygen [28], and also that anthracene's photodimerization rate increased at the silica gel–cyclohexane interface [29]. In both cases, the increased rates were explained as an effect of locally high concentrations. Kong and Ferry reported that the photodegradation rate of chrysene on laponite increased by a factor of approximately 10 in low ionic strength suspen-

sions, and that photodegradation was almost wholly dependent on the presence of oxygen [30]. Thomas reported that the rate of quenching of the excited state of immobilized pyrene and 1-pyrenebutyric acid on silica–air/liquid interfaces is reduced compared to the rate in the gas phase or in bulk solution [31,32]. The implication is that on surfaces, $^3\text{PAHs}$ may have longer lifetime and more chances to collide with a neighboring reactive species. Over the last 10 years, many other researchers have also reported surface mediated enhancement of photochemical processes, e.g., Takahashi et al. found that the photodegradation of the pyrethroid insecticide fenpropathrin was faster on soil than in water, with initial half-lives of 1–5 days on various soils versus >6 weeks in water [33]. Mathew and Khan reported that the photodegradation of metolachlor was faster in the presence

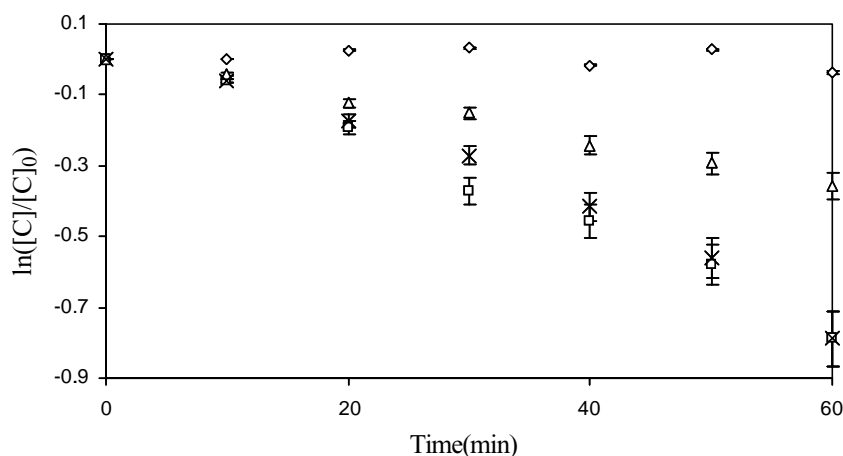


Fig. 2. The photolysis of chrysene is more rapid at the SiO_2 /water interface than in water. Conditions: 0.001 M NaHCO_3 buffer, pH: 8.30, $I_{\text{av}} = 2.60 \times 10^{-5} \text{ einstein min}^{-1}$; (Δ) 10% methanol solution, $k_{\text{obs}}: (0.60 \pm 0.06) \times 10^{-2} \text{ min}^{-1}$; (\times) SiO_2 suspension in 10% methanol, SiO_2 : 1 wt.%, $k_{\text{obs}}: (1.29 \pm 0.13) \times 10^{-2} \text{ min}^{-1}$; (\square) aqueous suspension of chrysene coated silica gel ($6.43 \mu\text{mol g}^{-1}$), SiO_2 : 1 wt.%, $k_{\text{obs}}: (1.31 \pm 0.13) \times 10^{-2} \text{ min}^{-1}$; (\diamond) aqueous suspension of silica coated with chrysene and DABCO (mole ratio: 1:10), SiO_2 : 1 wt.%.

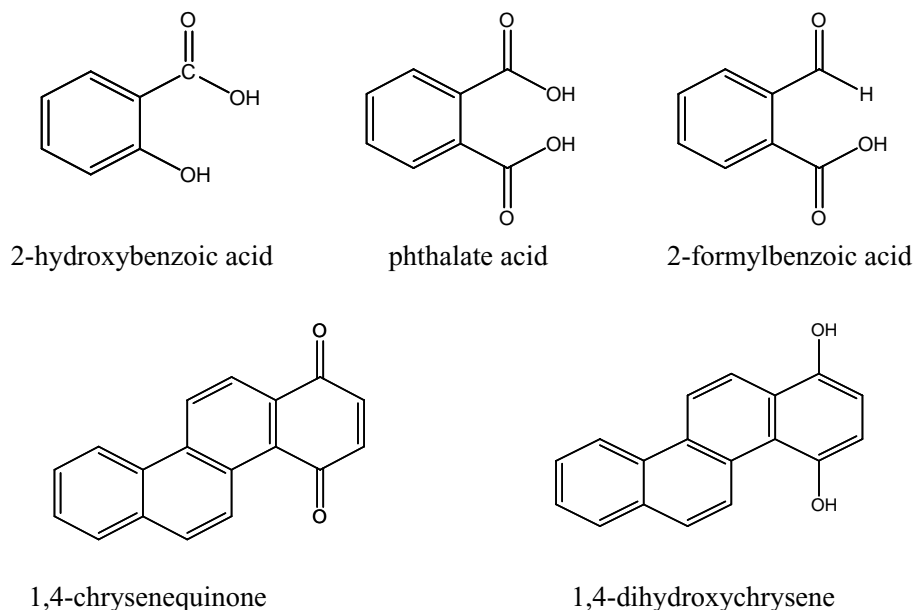


Fig. 3. Positively identified chrysene photooxidation products.

of clays (kaolinite, montmorillonite, and goethite) than in water [34]. In all cases, photolysis on surfaces was more rapid than in solution. Generally, this seems to hold true for hydrated surfaces also, although the rate enhancement may be somewhat less pronounced.

The addition of the singlet oxygen scavenger DABCO ([35], co-adsorbed) at a 10-fold excess (relative to chrysene) halted chrysene photodegradation completely. DABCO is known to react with singlet oxygen at the very high rate of $2.8 \times 10^8 \text{ l mol}^{-1} \text{ s}^{-1}$ [35]. Products were positively identified by comparison with standards, using GC–MS techniques (retention time, EI, CI, MS–MS) (Fig. 3). Products are consistent with those commonly observed from extensive PAH oxidation by singlet oxygen in water [6,38,39]. The mechanisms of photochemical degradation of PAHs in

solution include electron transfer [36–38] and self-sensitized oxidation by singlet oxygen [6,39,40], but our observation that DABCO inhibited chrysene oxidation suggests that $^1\text{O}_2$ is the most important removal mechanism in the $\text{SiO}_2/\text{H}_2\text{O}$ system. When the experiment was repeated with DABCO added directly to the aqueous phase instead of co-adsorbed it was just as effective at reducing the rate of photochemical oxidation, implying rapid equilibrium between the surface and solution. The photolysis rate of chrysene on the silica gel–water interface is very sensitive to chrysene loading, and the initial rate of chrysene photodegradation increased linearly with chrysene loading (Fig. 4). Although this observation is consistent with that expected from a self-sensitized process, it is not definitive; a similar result would be observed in the direct photolysis of optically thin solutions also.

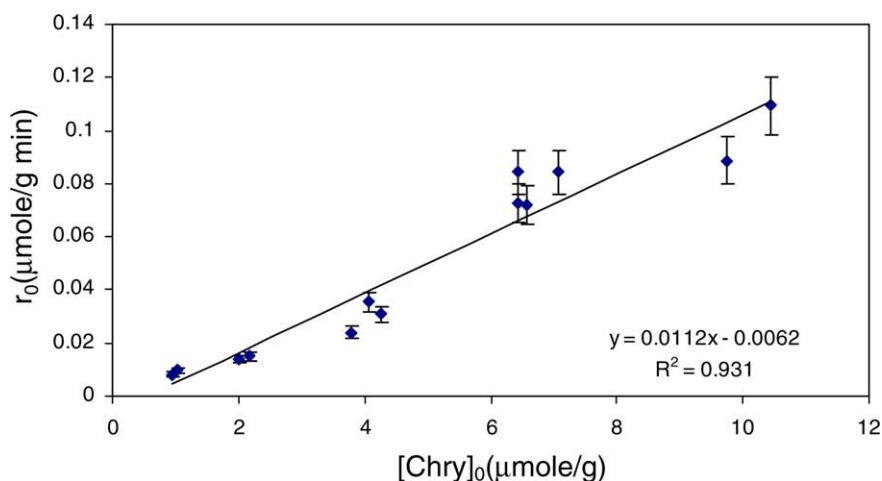


Fig. 4. The initial rate of chrysene photodegradation at silica gel–water interface varies as a function of initial loading of chrysene on silica gel. Conditions: 0.001 M NaHCO_3 , pH: 8.30, $I_{\text{av}} = 2.60 \times 10^{-5} \text{ einstein min}^{-1}$, SiO_2 : 1 wt.%.

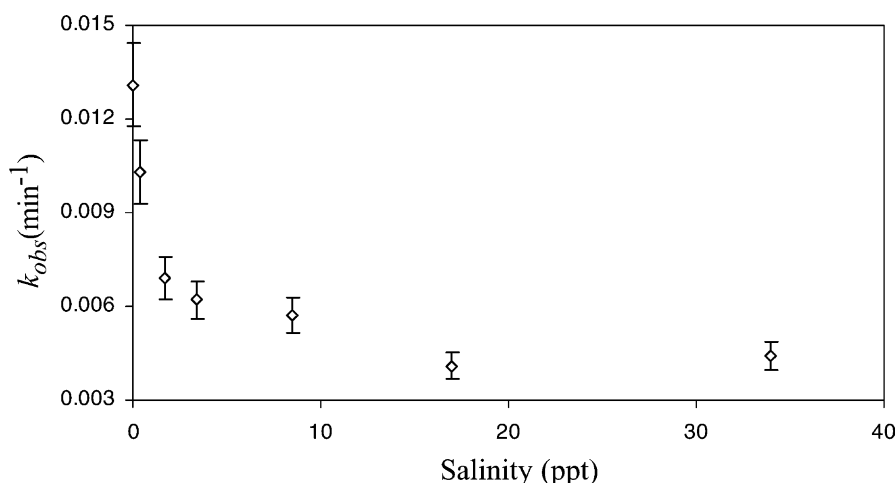


Fig. 5. Chrysene photodegradation rate falls off rapidly with increasing salinity pH: 8.30, $I_{av} = 2.60 \times 10^{-5}$ einstein min^{-1} , chrysene loading: $2.52 \mu\text{mol g}^{-1}$, SiO_2 : 1 wt.%.

3.3. The effect of salinity on the photodegradation rate of chrysene at the silica gel–water interface

The photolysis of chrysene at the silica gel–water interface was also studied as a function of salinity. The observed rate constant of chrysene degradation on silica gel decreased by a factor of 3, from $(1.31 \pm 0.13) \times 10^{-2}$ to $(0.44 \pm 0.04) \times 10^{-2} \text{ min}^{-1}$ as the salinity increased from 0 to 34 ppt (Fig. 5). This was expected that the given anions, Cl^- , Br^- , I^- in seawater can quench both excited state PAHs [41–43] and singlet oxygen [44–46]. However, the observation is significant because of what it implies about the photoreactivity of particulate bound PAHs in the environment. The observation suggests that the photodegradation of PAHs will fall off rapidly in coastal environments when suspended solids are transported from fresh water to seawater.

3.4. $[^1\text{O}_2]_{ss}$ determination

The disappearance of adsorbed chrysene was concentration dependent and could be halted by the singlet oxygen quencher DABCO, suggesting the principle reaction that accounted for the removal of chrysene was its oxidation by $^1\text{O}_2$ (Scheme 1). The rate of this process can be described by

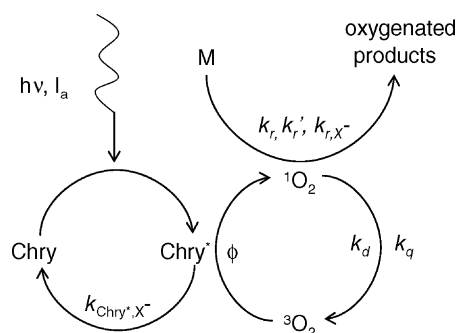
$$-\frac{d[\text{Chry}]}{dt} = k_r [^1\text{O}_2][\text{Chry}] \quad (1)$$

If the steady-state assumption is applied to $^1\text{O}_2$ in this system, a modified version of the method of Haag and Hoigne [30] can be used to quantify $[^1\text{O}_2]_{ss}$ (with a large excess of the $^1\text{O}_2$ trapping agent 2,5-diphenylfuran):

$$[^1\text{O}_2]_{ss} = \frac{k_{obs}}{k'_r} \quad (2)$$

where k_{obs} is the experimentally determined rate constant the loss of 2,5-diphenylfuran, and k'_r is the second order rate

constant of the reaction of 2,5-diphenylfuran with singlet oxygen ($k'_r = 4.6107 \text{ M}^{-1} \text{ s}^{-1}$ [47]). This method determines the averaged singlet oxygen concentration across the solution, and is not capable of measuring it directly on the silica surface or exclusively in solution. The steady state concentration of singlet oxygen increased with chrysene loading on silica gel in both 0.001 M NaHCO_3 buffer and simulated seawater suspensions (Fig. 6). In accordance with earlier observations on the effect of salinity on chrysene oxidation, $[^1\text{O}_2]_{ss}$ decreased by a factor of ~ 2.3 over the salinity range of 0–34 ppt, because of reaction between $^1\text{O}_2$ and the halides or because of quenching of photoexcited chrysene by halides. The effect of loading and salinity on $[^1\text{O}_2]_{ss}$ can be quantitatively predicted by



Scheme 1. I_a : the rate of light absorption by chrysene; ϕ : the quantum efficiency for sensitized $^1\text{O}_2$ production; M : probe substance (chrysene, 2,5-diphenylfuran, anions X^-); $k_d = 2.5 \times 10^5 \text{ s}^{-1}$ [49]: first-order rate constant for physical quenching of $^1\text{O}_2$ by water; k_q : the second-order rate constant for physical quenching of $^1\text{O}_2$ by the probe substance; k_r : the second-order rate constant for chemical reaction between $^1\text{O}_2$ and chrysene; $k'_r = 4.6 \times 10^7 \text{ M}^{-1} \text{ s}^{-1}$ [47]: the second-order rate constant for chemical reaction between $^1\text{O}_2$ and 2,5-diphenylfuran; k_{r,X^-} : the second-order rate constant for chemical reaction between $^1\text{O}_2$ and anions X^- ; $k_{\text{Chry}^*,\text{X}^-}$: the second-order rate constant for quenching/chemical reaction between excited state chrysene and X^- .

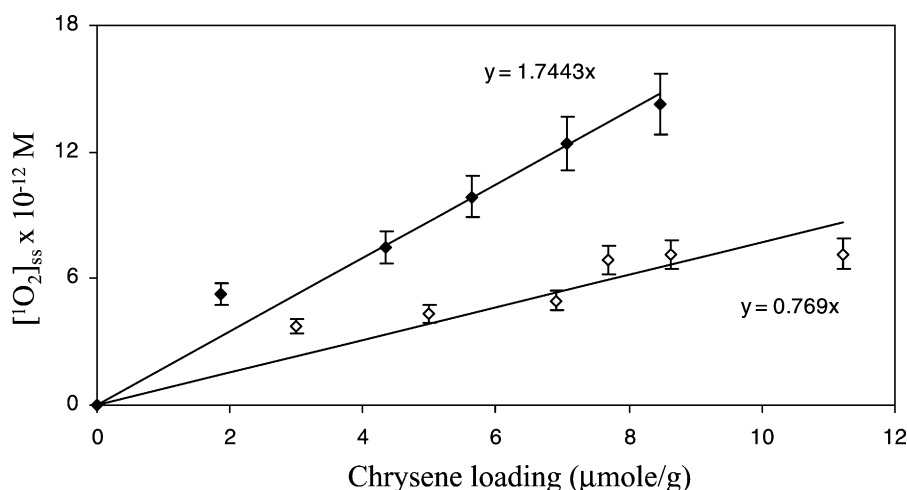


Fig. 6. $[^1\text{O}_2]_{\text{ss}}$ is a function of chrysene loading and salinity. Conditions pH: 8.30, $I_{\text{av}} = 2.60 \times 10^{-5}$ einstein min^{-1} , SiO_2 : 1 wt.%, (◆) 0 salinity, (◇) 34 ppt salinity.

Eq. (3) [48]:

$$[^1\text{O}_2]_{\text{ss}} = \frac{I_0 (1 - \sum (k_{\text{Chry}^*, \text{X}^-} [\text{X}^-])) \varepsilon b \phi [\text{Chry}]_0}{k_{\text{d}} + \sum (k_{\text{r}, \text{X}^-} [\text{X}^-])} \quad (3)$$

where I_0 is the light intensity, $k_{\text{Chry}^*, \text{X}^-}$ is the second-order rate constant for quenching of excited state of chrysene (both singlet and triplet) [41–43] by anions, k_{r, X^-} is the second order rate constant for quenching of $^1\text{O}_2$ by anions, $[\text{X}^-]$ is the concentration of anions and $[\text{Chry}]_0$ is the initial loading of chrysene on silica gel, ε is the molar extinction coefficient, b is the path length of the light in the solution, and ϕ is the quantum efficiency for sensitized $^1\text{O}_2$ production.

3.5. Conclusion

Our observations support a reaction manifold (Scheme 1) that includes the reactions between triplet chrysene and triplet oxygen to yield singlet oxygen, the oxidant that is primarily responsible for removing chrysene from the system. The results imply that PAHs associated with particulates and suspended solids may be more susceptible to photolysis than previously thought, although that removal process may be vulnerable to the presence of halide ions.

Acknowledgements

This research was sponsored by EPA-USA, Grant R827397. The authors would like to express gratitude to Prof. Catherine J. Murphy and Prof. Michael S. Angel for the use of spectroscopic equipment, and to the reviewers for helpful comments.

References

- [1] S.P. Zingg, M.E. Sigman, *Photochem. Photobiol.* 57 (3) (1993) 453–459.
- [2] J.T. Barbas, et al., *Photochem. Photobiol.* 58 (2) (1993) 155–158.
- [3] J.T. Barbas, R. Dabestani, M.E. Sigman, *J. Photochem. Photobiol. A: Chem.* 80 (1994) 103–111.
- [4] G.R. Helz, R.G. Zepp, D.G. Crosby (Eds.), *Aquatic and Surface Photochemistry*, Lewis Publishers, CRC Press, 1994, pp. 187–195.
- [5] G. Beck, J.K. Thomas, *Chem. Phys. Lett.* 94 (6) (1983) 553–557.
- [6] E. Lee-Ruff, H. Kazarians-Moghaddam, M. Katz, *Can. J. Chem.* 64 (7) (1986) 1297–1303.
- [7] R. Dabestani, K.J. Ellis, M.E. Sigman, *J. Photochem. Photobiol. A: Chem.* 86 (1995) 231–239.
- [8] M.E. Sigman, et al., *Environ. Sci. Technol.* 32 (24) (1998) 3980–3985.
- [9] M.E. Sigman, et al., *J. Photochem. Photobiol. A: Chem.* 94 (1996) 149–155.
- [10] K.-K. Iu, J.K. Thomas, *J. Photochem. Photobiol. A: Chem.* 71 (1993) 55–60.
- [11] M.P. Fasnacht, N.V. Blough, *Environ. Sci. Technol.* 36 (2002) 4364–4369.
- [12] K. Gollnick, *Adv. Chem. Ser.* 77 (1968) 78–101.
- [13] M.E. Sigman, et al., *Tetrahedron Lett.* 32 (41) (1991) 5737–5740.
- [14] J.K. Thomas, E.H. Ellison, *Adv. Colloid Interface Sci.* 89–90 (2001) 195–238.
- [15] K. Takagi, Y. Sawaki, *Crit. Rev. Biochem. Mol. Biol.* 28 (4) (1993) 323–367.
- [16] B. Stevens, *Acc. Chem. Res.* 6 (1973) 90–96.
- [17] B. Stevens, S.R. Perez, J.A. Ors, *J. Am. Chem. Soc.* 96 (1974) 6846–6850.
- [18] N.J. Turro, Addison-Wesley, Reading, MA, 1978 (Chapter 14).
- [19] K.P.C. Vollhardt, *Organic Chemistry*, Freeman, New York, 1987.
- [20] D. Li, J. Park, J.R. Oh, *Anal. Chem.* 73 (13) (2001) 3089–3095.
- [21] C.A. Reyes, et al., *Environ. Sci. Technol.* 34 (3) (2000) 415–421.
- [22] J.S. Miller, D. Olejnik, *Water Res.* 35 (1) (2001) 233–243.
- [23] F. Ngan, T. Ikesaki, *J. Chromatogr.* 537 (1–2) (1991) 385–395.
- [24] M. Anpo, H. Nishiguchi, T. Fujii, *Res. Chem. Intermed.* 13 (1) (1990) 73–102.
- [25] R.K. Bauer, et al., *J. Phys. Chem.* 86 (19) (1982) 3781–3789.
- [26] S.A. Ruetten, J.K. Thomas, *J. Phys. Chem. B* 102 (1998) 598–606.
- [27] R.S. Pearlman, S.H. Yalkowsky, S. Banerjee, *J. Phys. Chem. Ref. Data* 13 (2) (1984) 555–562.
- [28] M.E. Sigman, S.P. Zingg, in: D.G. Crosby (Ed.), *Aquatic and Surface Photochemistry*, Lewis Publishers, Boca Raton, 1994, pp. 197–206.
- [29] M.E. Sigman, R. Dabestani, E. Hagaman, 225th ACS National Meeting, New Orleans, LA, USA, 2003.
- [30] W.R. Haag, J. Hoigne, *Environ. Sci. Technol.* 20 (1986) 341–348.

- [31] S.A. Ruetten, J.K. Thomas, *J. Phys. Chem. B* 103 (8) (1999) 1278–1286.
- [32] R.J. Kavanagh, J.K. Thomas, *Langmuir* 14 (1998) 352–362.
- [33] N. Takahashi, et al., *Pest. Sci.* 16 (2) (1985) 119–131.
- [34] R. Mathew, S.U. Khan, *J. Agric. Food Chem.* 44 (1996) 3996–4000.
- [35] Y. Lion, E. Gandin, A. Van de Vorst, *Photochem. Photobiol.* 31 (4) (1980) 305–309.
- [36] R.A. Larson, L.L. Hunt, D.W. Blankenship, *Environ. Sci. Technol.* 11 (1977) 492–496.
- [37] R.A. Larson, et al., *Environ. Sci. Technol.* 13 (1979) 965–969.
- [38] C.X. Wang, et al., *Chemosphere* 30 (3) (1995) 501–510.
- [39] W.C. Eisenberg, M. Desilva, *Tetrahedron Lett.* 31 (41) (1990) 5857–5860.
- [40] W.C. Eisenberg, et al., *Photochem. Photobiol.* 56 (4) (1992) 441–445.
- [41] W. Fenical, D.R. Kearns, P. Radlick, *J. Am. Chem. Soc.* 91 (1969) 7771.
- [42] G.G. Aloisi, G. Favaro, *J. Chem. Soc., Perkin Trans. II* 4 (1976) 456–460.
- [43] G. Knor, *Chem. Phys. Lett.* 330 (2000) 383–388.
- [44] I. Rosenthal, A. Frimer, *Photochem. Photobiol.* 23 (3) (1976) 209–211.
- [45] K.K. Rohatgi-Mukherjee, A.K. Gupta, *Chem. Phys. Lett.* 46 (2) (1977) 368–371.
- [46] S.Y. Egorov, A.A. Krasnovsky, *Sov. Plant Physiol.* 33 (1) (1986) 5–8.
- [47] R.H. Young, D. Brewer, R.A. Keller, *J. Am. Chem. Soc.* 95 (2) (1973) 375–379.
- [48] L. Kong, J.L. Ferry, *Environ. Sci. Technol.*, 2003, in press.
- [49] M.A.J. Rodgers, P.T. Snowden, *J. Am. Chem. Soc.* 104 (1982) 5541–5543.